# I-123 HIPDM Brain Imaging with a Rotating Gamma Camera and Slant-Hole Collimator

Joseph F. Polak, B. Leonard Holman, Jean-Luc Moretti, Robert L. Eisner, John Lister-James, and Robert J. English

*Harvard Medical School, Boston, Massachusetts, and The General Electric Company, Milwaukee, Wisconsin*

**The performance of a slant-hole collimator was compared with that of a standard straight-bore, low-energy collimator for tomographic imaging of I-123-iodinated amine brain agents. Improved in-slice resolution was due to the greater proximity between collimator and the subjects' heads. We conclude that high quality tomographic images of the brain can be obtained from rotating cameras equipped with slant-hole collimators.**

J Nucl Med 25: 495–498, 1984

A major disadvantage to tomographic imaging of the brain with the rotating gamma camera is the need for the detector to clear the patient's shoulders (Table 1). Considerable space is needed between the collimator face and the brain, with a consequent decrease of resolution (*1*). There are at least three ways to mitigate this problem. The first is to use a rotating camera whose crystal surface occupies a greater portion of the leading edge of the camera, thus permitting movement around the head at a reduced radius. The second is to use a camera able to follow the body contour (*2*). Although this might improve resolution along the anteroposterior axis, the collimator must still clear the patient's shoulders on both sides. The third solution is to use a slant-hole collimator arranged in such a way that the septa are perpendicular to the axis of rotation of the camera (*3*). Thus, since only the farthest edge of the camera must clear the shoulders, the resolution in the plane of the orbitomeatal line is improved.

We have evaluated the applicability of slant-hole collimation for imaging amines labeled with I-123 ($p,2n$). Despite I-124 contamination (2% to 4%), images of high quality can be obtained with a gain in resolution over images obtained with standard straight-bore collimators.

## METHODS

**Tracer.** All I-123* imaging experiments were conducted with less than 5% I-124 contamination.

**Equipment and phantoms.** A rotating tomographic camera and computer† were used to acquire and process the tomographic data sets.

Two collimators were used: a low-energy, general-purpose (LEAP) and a modified slant-hole collimator. Both are slightly over 4 cm thick and are manufactured by casting (Table 2).

A cylindrical, water-filled phantom (diam 20 cm), containing centrally and peripherally located line sources, was used to assess in-plane resolution for both collimators. The "lines" used were polyethylene tubing with i.d. 0.58 cm. Specific activity was kept at over 4 mCi/ml.

Planar images were stored in a 128 × 128 matrix, with the same geometry used for patient imaging. For the LEAP, the radius of rotation was 22 cm. The slant-hole was tilted (Fig. 1), giving clearances between 2 and 22 cm and estimated radii ranging from 10 cm to 14 cm at the orbitomeatal line. Proper alignment of the slant-hole collimator was verified by plotting the trajectory of a Co-57 point source on the camera crystal as a function of the angular position of the camera head. Optimal angulation of the camera head resulted in a trajectory limited to only one plane of the y axis (axis corresponding to the long axis of a subject; referred to as YC in Figure 2). The center of rotation was then calculated using standard quality control procedures for the computer system.

**TABLE 1. ESTIMATED RADII OF ROTATION FOR A PATIENT POPULATION SEEN IN A NUCLEAR MEDICINE UNIT***

| Number | Sex | Age (range) | Radius of rotation (mean) | Radius of rotation (range) |
|---|---|---|---|---|
| 10 | F | 23–78 yr | 19.6 ± 0.8 cm | 18.3–21.0 cm |
| 10 | M | 49–83 yr | 22.0 ± 0.9 cm | 10.6–23.5 cm |

* Calculated from measured shoulder breadths.

Received Sept. 7, 1983; revision accepted Nov. 15, 1983.

For reprints contact: B. Leonard Holman, MD, Dept. of Radiology, Harvard Medical School, 25 Shattuck St., Boston, MA 02115.

**TABLE 2. COLLIMATOR CHARACTERISTICS**

| Type | Hole diameter | Type | Septal thickness | Hole length | No. of holes | Field of view |
|---|---|---|---|---|---|---|
| Slant-hole | 2.5 mm | Hex | 0.3 mm | 40.4 mm | 18,000 | 400 mm |
| LEAP | 2.6 mm | Round | 0.3 mm* | 40.0 mm | 15,000 | 400 mm |

* Minimal thickness.

Verification of the exactness of this center of rotation value for different tomographic cuts was made by imaging two parallel Tc-99m line sources in air, one at the center of rotation, the other 10 cm distant, and reconstructing tomographic slices over the length of the collimator. The lack of change in the xy coordinates of these tomographic line-source images for the different tomographic slices verified the proper angulation of the gantry and of the camera head. Values of full width at half maximum (FWHM) were calculated for the tomographic levels corresponding to the transaxial images acquired in patients.

**Patient imaging.** Imaging began 20 min after i.v. injection of I-123-labeled HIPDM‡ (*4*). Acquisitions were made over 64 angular projections (360°) at 25 sec to 40 sec per projection. A 64 × 64 matrix format was applied over the 40-cm field of view, yielding pixel sizes and a slice thickness of 6.3 mm. Paired studies were made on the same patient, before and after collimator change. The collimator used first was randomly determined. Imaging time depended on the patient's clinical status (Table 3).

**Data processing.** Transaxial reconstructions were made by filtered back-projection using a pure ramp filter. A three-dimensional Hanning filter was then applied to points in the plane of the reconstruction and neighboring points in the two adjacent slices.

Relative target-to-nontarget ratios for the two collimators were estimated by measuring total counts recorded from the brain divided by those outside, on both planar images and reconstructed tomograms taken at the same level. Regions of interest of similar size were used.

Three observers, unaware of which collimator was used, reviewed the two transaxial data sets for each patient and scored image quality on a 3-point scale: worse, equal to, or better.

**Statistical analysis.** All results are reported as mean ± standard deviation.

## RESULTS

**Phantom studies.** After tomographic reconstruction, the FWHM values at the center of the water-filled phantom were slightly less for the slant-hole collimator than for the LEAP. Each FWHM was calculated at the same radius of rotation observed during patient imaging. The FWHM for the slant-hole collimator values were 1.8 cm and 2.0 cm for radii of 15 cm and 18 cm, respectively, whereas the FWHM values for the general-purpose collimator was 2.0 cm at an orbiting radius of 22 cm.

Planar FWHM values for the LEAP were 1.2 and 1.6 cm, and were 1.3 and 1.5 cm for the slant-hole collimator at distances of 15 and 20 cm, respectively.

**Patient imaging.** Tomographic imaging times varied between 25 min and 40 min, the shortest being for the patient with a recent cerebrovascular accident (No. 3, Table 3).

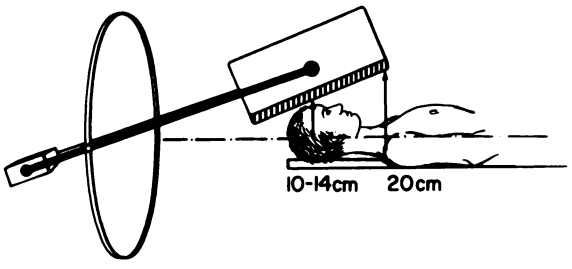


**FIG. 1.** Typical arrangement of rotating gamma camera equipped with slant-hole collimator. Central holes are perpendicular to axis of rotation and remain so during complete 360° cycle. Ideally, radii of revolution <14 cm should be attainable.

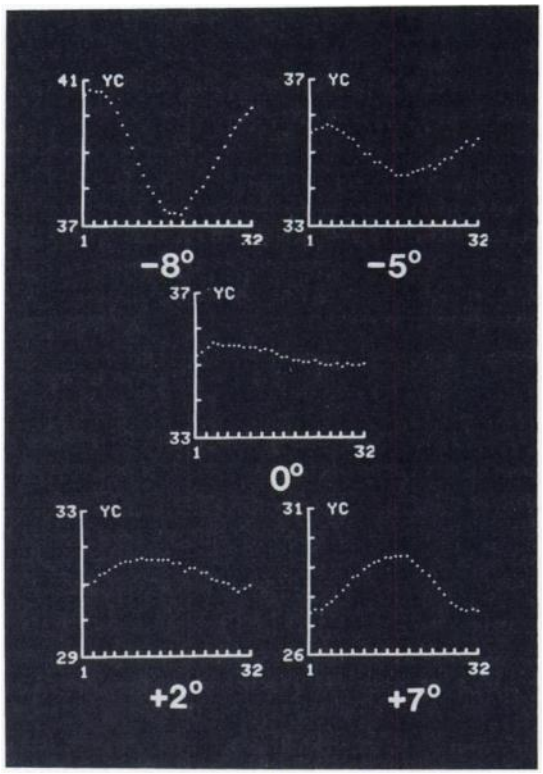


**FIG. 2.** The trajectory of Co-57 point source on crystal face of rotating gamma camera is plotted as function of angular position during full rotation of camera. Excursions along presumed long axis of patient (y axis referred to as YC in figure) are used to verify proper angulation of camera head. At ideal position (0°), collimator holes are perpendicular to axis of rotation: point source image remains within same tomographic plane (YC value). As camera head is angled caudad (−5° and −8°) or cephalad (+2° and +7°), excursion of point source crosses into other tomographic planes corresponding to different YC values. Angles shown are related to resting angle of 26.6° for camera head with respect to horizontal (Fig. 1).

**TABLE 3. COMPARISON OF LOW-ENERGY GENERAL-PURPOSE AND SLANT-HOLE COLLIMATORS**

| Patient No. | Clinical status | Dose (mCi) | Time/projection (sec) | | Counts in brain per projection | | Counts in brain after tomographic reconstruction | | Background counts (as % of total counts in brain) | | | |
|---|---|---|---|---|---|---|---|---|---|---|---|---|
| | | | | | | | | | Planar images | | Tomographic slices | |
| | | | LEAP | Slant | LEAP | Slant | LEAP | Slant | LEAP | Slant | LEAP | Slant |
| 1 | Normal | 5.7 | 40 | 40 | 17793 | 32121 | 60809 | 70494 | 35.2 | 44.5 | 7.2 | 6.0 |
| 2 | Normal | 4.9 | 30 | 30 | 15638 | 26400 | 47872 | 61482 | 32.1 | 41.4 | 10.5 | 17.2 |
| 3 | Right C.V.A. | 5.0 | 30 | 25 | 12811 | 17483 | 30211 | 33142 | 49.0 | 57.2 | 13.8 | 22.2 |
| 4 | Normal | 5.0 | 30 | 30 | 11932 | 19542 | 34537 | 39965 | 30.4 | 46.6 | 12.0 | 17.8 |
| 5 | Normal | 5.0 | 30 | 30 | 15186 | 25441 | 44622 | 54441 | 39.1 | 45.3 | 8.6 | 14.2 |
| | | | | | | | | | 37.2 ± 7.4% | 47.0 ± 6.0% | 10.4 ± 2.6% | 15.5 ± 6.0% |

**TABLE 4. OBSERVERS' JUDGMENTS OF IMAGE QUALITY IN TOMOGRAPHIC RECONSTRUCTIONS**

| Number | % | Judgment |
|---|---|---|
| 11 | 73% | Slant better than LEAP |
| 3 | 20% | Slant equal to LEAP |
| 1 | 7% | Slant not as good as LEAP |
| 15* | | |

* Three observers judging five images each.

On the planar images there was significantly more background with the slant-hole collimator than with the LEAP (47.0% compared with 37.2%; Table 3).

After tomographic reconstruction, the slant-hole collimator provided more counts per cerebral slice, but background was higher (15.5% compared with 10.4%, Table 3). Regarding overall image quality, the three observers found that the reconstructed slant-hole images were either better than those obtained with the LEAP (73%) or at least as good (20%) (Table 4). Image contrast, particularly between gray and white matter was significantly improved with the slant-hole collimator (Fig. 3).

## DISCUSSION

The problems encountered during our study were threefold: the geometry of the slant-hole collimator adapted to a rotating gamma camera; I-124 contamination; I-123; and the choice of a digitizing

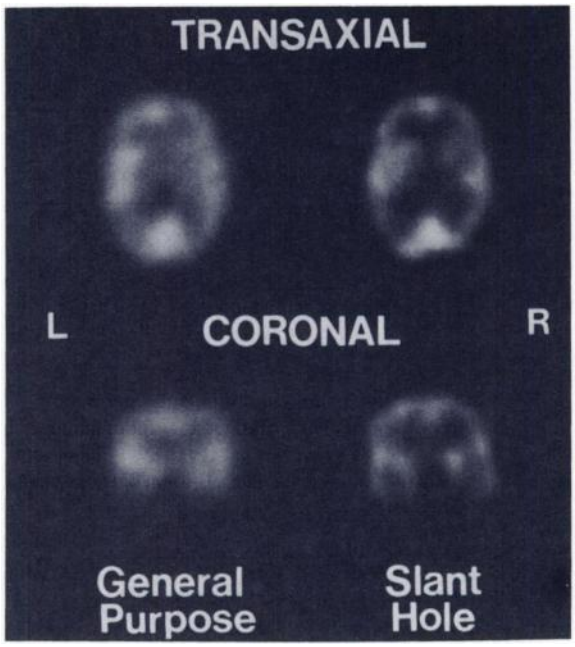


**FIG. 3.** Comparison of HIPDM patient images (slice thickness 6.3 mm) obtained with slant-hole and low-energy general-purpose (LEAP) collimators. Transaxial slices taken at level of basal ganglia confirm that slant-hole offers better image quality. On coronal slices, temporal horns are shown better with slant-hole collimator; there is also better delineation of periventricular white matter.

interval (matrix size) sufficient to preserve the gain in spatial frequencies offered by the slant-hole collimator.

As with the straight-bore collimator, the rotation of the camera assembly must define a series of parallel planes perpendicular to the axis of revolution. With the slant-hole collimator, the camera head must be angled in such a way that the collimator holes remain perpendicular to the axis of rotation (long axis of the subject, Fig. 1) during tomographic acquisitions. This angle was determined experimentally since, in our case, the specified angle of 30° for our prototype collimator was in error by 3.4°. In order to correctly position the camera head, we use the same quality control algorithms implemented for standard tomographic imaging with straight-bore collimators. The trajectory made by a Co-57 point source on the camera face during a full rotation of the gantry was plotted as a function of angular projection for both the x and y axis of the camera. Trajectories in the y direction (long axis of the subject in Fig. 1; YC in Fig. 2) reach a minimum amplitude when the collimator holes are perpendicular to the axis of rotation of the gantry. In our case, this angle of 26.6° is measured between the camera face and the horizontal. The more the camera head in Fig. 1 is angled either forward or backward, the larger the trajectory made in the y axis (YC in Fig. 2) and the more degraded the tomographic reconstructions due to superposition of data from adjacent slices.

Brain imaging with labeled amines has been performed using pure I-123 ($p$,5$n$) as the tracer (*5-8*), especially in Europe. With I-123 produced by the $p$,2$n$ reaction, contamination of the I-123 with I-124 can be a problem, requiring thicker collimators to control the higher-energy photons (*10*). In this study we have compared collimators with similar septal thickness (Table 2). Some of the increased counts observed with the slant-hole collimator (Table 3) must be due to penetrating radiations from the torso (Fig. 1). The detector's axis points toward lungs and liver, two of the primary sites where these compounds are taken up (*4*).

Although the planar resolution of the slant-hole is significantly improved at the collimator-to-target distances seen during patient imaging (FWHM = 1.3 cm compared with 1.6 cm for the slant-hole at 15 cm and the LEAP at 20 cm), the measurements made on the reconstructed slices (1.8 cm compared with 2.0 cm for the slant-hole at 15 cm radius of rotation and the LEAP 22 at cm) underestimate this difference. The most plausible explanation for this effect is undersampling of the camera's field of view. The importance of a matrix sufficiently fine to preserve the spatial frequencies contained in planar images is well known (*11*). Similar observations recently made regarding tomographic imaging indicate that the gain in resolution achieved with the slant-hole collimator can be fully appreciated only with a finer (128 × 128 matrix) digitizing interval (*1,12*).

Despite these limitations, we have shown that the images obtained with the slant-hole collimator are at least equivalent to or better than those of the LEAP (straight-bore) collimator in 93% of cases (Table 4). We therefore conclude that brain imaging using HIPDM labeled with I-123 ($p$,2$n$) is feasible using the slant-hole collimator and a rotating gamma camera.

## FOOTNOTES

* Medi-Physics, Inc., Emeryville, California.

† General Electric 400T, General Electric Company, Medical Imaging Systems, Milwaukee, Wisconsin.

‡ N,N,N′-trimethyl-N′-[2-hydroxyl-3-methyl-5-(I-123)iodobenzyl]-1,3-propanediamine.

## ACKNOWLEDGMENTS

The authors thank Monte Blau, Ph.D. and H. Kung, M.D. of SUNY at Buffalo, New York, for supplying nonradioactive HIPDM kits. We also thank Mrs. Margaret J. R. Senechal for her valuable assistance throughout the preparation of this manuscript.

## REFERENCES

1. LARSSON SA: Gamma camera emission tomography. *Acta Radiol* (Suppl) 363:1-75, 1980
2. KING MA, SCHWINGER RB, ESSER PD, et al: Preliminary characterization of the properties of a new rotating SPECT imaging system. In *Emission Computed Tomography—Current Trends*. Esser PD, ed. New York, Society of Nuclear Medicine, 1983, pp 91-104
3. ESSER PD, MITNICK RJ, ARLISS J, et al: Angular single photon emission computed tomography (SPECT): An improved method for cranial tomographic imaging. *J Nucl Med* 24:P75, 1983 (abst)
4. HOLMAN BL, LEE RGL, HILL TC, et al: A comparison of two cerebral blood flow tracers, N-isopropyl I-123 p-iodoamphetamine and I-123 HIPDM. *J Nucl Med* 24:P6, 1983 (abst)
5. MORETTI JL, ASKIENAZY S, RAYNAUD C, et al: La N-isopropyl-*p*-iodoamphetamine I-123 en tomoscintigraphie cérébrale. *Ann Radiol* 26:59-67, 1983
6. FAZIO F, GERUNDINI P, LENZI GL, et al: Evaluation of cerebrovascular disorders using the brain imaging agent, (I-123) HIPDM, and single photon emission computed tomography (SPECT). *J Nucl Med* 24:P5, 1983 (abst)
7. COLEMAN RE, GREER KL, DRAYER BP, et al: Collimation of I-123 imaging with SPECt. In *Emission Computed Tomography—Current Trends*. Esser PD, ed. New York, Society of Nuclear Medicine, 1983, pp 135-145
8. CLARKE LP, VAUGHAN S, HOURANI M, et al: Collimator choice for differential uptake measurements using SPECT imaging with I-123. *J Nucl Med* 24:P75, 1983 (abst)
9. HILL TC, HOLMAN BL, LOVETT RD, et al: Initial experience with SPECT (single-photon computerized tomography) of the brain using N-isopropyl I-123 p-iodoamphetamine: Concise communication. *J Nucl Med* 23:191-195, 1982
10. POLAK JF, HOLMAN BL, ENGLISH RJ: Performance of collimators used for tomographic imaging of I-123 contaminated with I-124. *J Nucl Med* 24:1065-1069, 1983
11. BRILL AB, ERICKSON JJ: Factors affecting the collection and analysis of radiotracer images. *Semin Nucl Med* 3: 285-300, 1973
12. HAERTEN RL, BIESZK JA, HAWMAN EG, et al: Evaluation of SPECT system performance using a SPECT phantom. *J Nucl Med* 24:P58, 1983 (abst)